JOURNAL OF AIRCRAFT
Vol. 30, No. 1, Jan.–Feb. 1993

Wavelet Analysis of Gust Structure in Measured Atmospheric Turbulence Data

J. G. Jones,* G. W. Foster,† and P. G. Earwicker†
Defense Research Agency, RAE Farnborough, Hampshire GU14 6TD, England, United Kingdom

A method for analyzing atmospheric turbulence data is described in the form of a wavelet analysis which extracts localized structure in the form of discrete ramp-shaped gusts. A two-dimensional correlation surface is generated, the independent variables being position and scale, and discrete gusts are detected by the identification of peaks in this correlation surface which is equivalent to the invertible wavelet transform (WT). This method is illustrated by application to measured turbulence records. Implications of the results for aircraft-design criteria, particularly for structural loads and load-alleviation control systems, are discussed.

Introduction

THE traditional basis for analyzing fluctuating data—such as atmospheric-turbulence measurements—has been Fourier analysis, the typical analysis product taking the form of power-spectral densities. However, it has become apparent that power-spectral densities have limitations as a basis for the representation of fluctuating phenomena that contain strongly localized events. The localization of structure in a random process is a consequence of phase correlation, which is not taken into account by the power-spectral density. As a result, new methods [particularly the wavelet transform (WT)[1,2]] have recently been developed which provide an alternative representation of localized structure, using position and scale as independent variables.

Whereas Fourier analysis is implemented by correlating the data with a succession of sinusoidal waves of differing phase and frequency, wavelet analysis is performed by correlating the data with a set of strongly-localized functions (analyzing wavelets) of constant shape but covering a range of positions and scales.

This article describes a new method of wavelet analysis in the form of multiresolution correlation detection[3] of localized events or structures. In standard correlation detection a correlation filter is translated with respect to the data, and localized events are detected by the identification of correlation peaks. Here, the translation of the filter is generalized to include both translation and change of scale (zoom), and localized events or structures are detected by the identification of peaks (maxima or minima) in a two-dimensional correlation surface parameterized by position and scale. Formally, the correlation surface is equivalent to the WT. Whereas the entire correlation surface contributes to the invertible WT, only the surface in the vicinity of local maximum and minimum values contributes to correlation detection.

Although the step of calculating the correlation surface is linear, the process of extracting structure associated with peaks in the surface is essentially nonlinear. The two steps (of calculating the transform and of extracting peaks) are somewhat analogous to the calculation of Fourier transforms and subsequent extraction of spectral lines. In each case the result is a representation which is not completely invertible, but which economically captures the essential aspects of structure.

Multiresolution Correlation Detection

The problem of correlation detection can be formulated as follows: measured data are assumed to be available in the form of a real function $g(x)$ over a finite domain. In the present context $g(x)$ is taken to be a one-dimensional fluctuating component of turbulence velocity. It is expressed as the sum

$$g(x) = f(x) + n(x) \tag{1}$$

of a discrete "signal" $f(x)$, chosen to have a prescribed deterministic waveform, and a Gaussian residual "noise" $n(x)$. In the standard theory of correlation detection $n(x)$ is assumed to be white. Here the noise is generalized to be self-similar, or rather self-affine,[4] and exhibits a power-law spectrum of the form

$$\phi_h(\omega) \propto |\omega|^{-(2h+1)} \tag{2}$$

where the constant h is a scaling, or "similarity" parameter. By assuming the value $h = \frac{1}{3}$, the spectrum takes the form $|\omega|^{-5/3}$, corresponding to the "inertial" range of frequencies in the von Karman spectrum.

The signal $f(x)$ is assumed to be of prescribed shape but of unknown position and scale. It may thus be expressed in terms of a single function $\bar{f}$ in the form

$$f(x) = \bar{f}[(x - y)/L], \qquad (L > 0) \tag{3}$$

where $f(x)$ is obtained from $\bar{f}$ through the successive operations of scaling, or dilation, by L and translation by y.

The optimum detection of $f(x)$ [Eq. (3)] in data $g(x)$ [Eq. (1)] with the noise $n(x)$ having a power-spectrum given by Eq. (2), is achieved[3] by maximizing simultaneously with respect to y and L the function

$$T_h(y, L) = L^{-(h+1)} \int_{-\infty}^{\infty} \bar{F}[(x - y)/L] g(x)\, dx \tag{4}$$

The correlation filter, or analyzing wavelet $\bar{F}$ is evaluated[3] as the convolution

$$\bar{F}(x) = w_h * \bar{f} \tag{5}$$

of $\bar{f}$ by the function w_h whose Fourier transform is given by

$$\hat{w}_h(\omega) = [\phi_h(\omega)]^{-1} \tag{6}$$

Presented as Paper 91-0448 at the AIAA 29th Aerospace Sciences Meeting, Reno, NV, Jan. 7–10, 1991; received Feb. 4, 1991; revision received Jan. 24, 1992; accepted for publication Jan. 25, 1992.

*Senior Principal Scientific Officer. Member AIAA.
†Principal Scientific Officer.

and ϕ_h is given by Eq. (2). Furthermore, if an arbitrary (positive) amplitude factor m is incorporated in the right side of Eq. (3), then an estimate of m is given by the value of $L^h[T_h(y, L)]_{max}$.

If multiple copies of the discrete signal profile $\bar{f}$ exists in the data, then locally maximum values, or peaks, in the two-dimensional surface $T_h(y, L)$ determine the estimated positions, scales, and amplitudes of these copies.

Comparison with Wavelet Transform

The expression for $T_h(y, L)$ [Eq. (4)] is formally identical to the invertible WT of $g(x)$ with respect to the analyzing wavelet $\bar{F}(x)$. Applications have been published of the WT to seismic signals[1] and sound patterns.[2]

Since the WT is invertible, no information is lost in making the transformation; the function can be reconstructed exactly from $T_h(y, L)$. In the interpretation in terms of correlation detection just the information contained in the locally maximum (and minimum) values of $T_h(y, L)$ is extracted.

Associated with this change in interpretation is a difference between the necessary conditions imposed on the analyzing wavelet $\bar{F}(x)$. For interpretation as a WT, necessary conditions on $\bar{F}(x)$ include[2] both

$$\int |\bar{F}(x)|^2 \, dx < \infty \tag{7}$$

(finite energy) and

$$\int \bar{F}(x) \, dx = 0 \tag{8}$$

(zero mean).

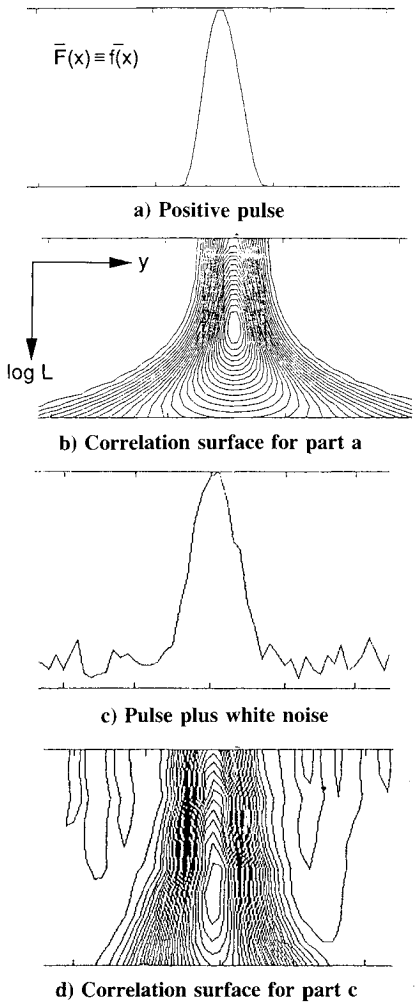

a) Positive pulse

b) Correlation surface for part a

c) Pulse plus white noise

d) Correlation surface for part c

Fig. 1 Detection of positive pulse.

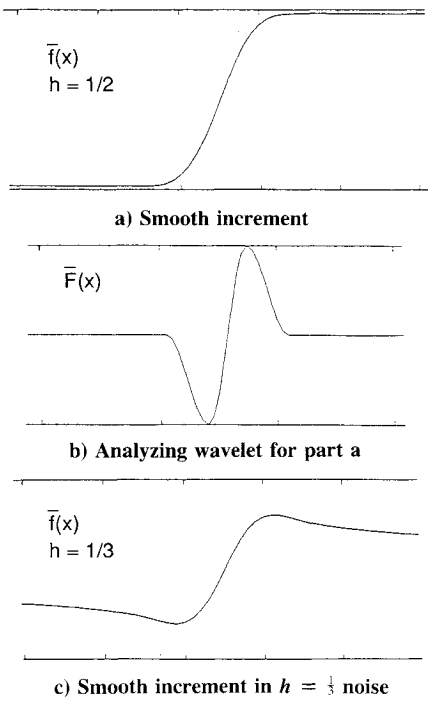

a) Smooth increment

b) Analyzing wavelet for part a

c) Smooth increment in $h = \frac{1}{3}$ noise

Fig. 2 Detection of ramp-shaped discrete gust

For Eq. (4) to be used in correlation detection, the admissibility constraint on $\bar{F}(x)$ can be expressed[3] in the form

$$\int_{-\infty}^{\infty} W_h^{-1}\bar{F}(x) \cdot \bar{F}(x) \, dx < \infty \tag{9}$$

where W_h is the positive definite operator whose application to a function s can be expressed as convolution by w_h [Eq. (6)]:

$$W_h s = w_h * s \tag{10}$$

In particular, from Eq. (5)

$$\bar{F}(x) = W_h \bar{f}(x) \tag{11}$$

When the noise $n(x)$ is white, $h = -\frac{1}{2}$, $W_h \equiv I$, and Eq. (9) becomes identical to Eq. (7). The constraint imposed by Eq. (8) is not required in correlation detection. This in particular allows the detection of a positive pulse $\bar{f}(x)$ (Fig. 1a) in white noise, for which $\bar{F}(x) \equiv \bar{f}(x)$ and Eq. (8) is violated. Furthermore, when the noise has a spectrum corresponding to that of turbulence in the inertial range of the von Karman spectrum, it allows the detection of a smooth ramp profile (Fig. 2c).

Extraction of Elementary Features

Consider first the case in which the noise $n(x)$ [Eq. (1)] is white. Then $\bar{f}(x)$ can be chosen to be a positive pulse of finite energy (Fig. 1a). The constraint [Eq. (9)] is satisfied since

$$\int_{-\infty}^{\infty} W_h^{-1}\bar{F}(x) \cdot \bar{F}(x) \, dx = \int_{-\infty}^{\infty} |\bar{f}(x)|^2 \, dx < \infty \tag{12}$$

When the noise amplitude is infinitesimally small the associated correlation surface [Eq. (4)], is as illustrated in Fig. 1b, and comprises a positive function characterized by a single maximum value from which the position y, scale L and amplitude of the pulse can be inferred. The effect of finite-amplitude white noise is shown in Figs. 1c and 1d.

More relevant to the analysis of atmospheric turbulence is the situation in which the measured fluctuations $g(x)$ [Eq. (1)] exhibit a power-law spectral density which is closer to

$1/|\omega|^2$ than white, or constant. A discrete data decomposition may be performed in this case by assuming for the residual $n(x)$ a power-law spectrum [Eq. (2)], at least approximately equal to that of the measured data. Assuming, in particular, the noise spectrum to be proportional to $|\omega|^{-2}$, the scaling parameter takes the value $h = \frac{1}{2}$. It follows from Eq. (10) that the operator W_h is given by

$$W_{1/2} = \frac{-\mathrm{d}^2}{\mathrm{d}x^2} \tag{13}$$

Furthermore, the constraint given by Eq. (9) translates [using Eqs. (11) and (13)] into an equivalent constraint

$$\int_{-\infty}^{\infty} \left(\frac{\mathrm{d}\bar{f}}{\mathrm{d}x}\right)^2 \mathrm{d}x < \infty \tag{14}$$

on the feature profile $\bar{f}(x)$. The most elementary discrete signal component which satisfies this constraint is that whose derivative is a discrete pulse (as in Fig. 1a) of finite energy. Such a profile $\bar{f}$ takes the form of a "smooth increment," Fig. 2a, which is the present context may be interpreted as a ramp-shaped discrete gust, like that used in the statistical-discrete-gust method.[5-7]

The associated analyzing wavelet $\bar{F}(x) = [-(\mathrm{d}^2\bar{f}/\mathrm{d}x^2)](x)$ [from Eqs. (11) and (13) illustrated in Fig. 2b], can be implemented as the convolution of a pair of delta functions of opposite sign with a smoothing filter. The filter whose weighting function is such a pair of delta functions is a "differencing" filter, and its combination with a smoothing operation to give the analyzing wavelet in Fig. 2b, produces a "smoothed difference" filter. Applications of this filter to the analysis of measured turbulence records have been described previously in Refs. 8 and 9.

The correlation surface [Eq. (4)] that results when the analyzing wavelet in Fig. 2b is applied to the smooth increment (Fig. 2a) again comprises a positive function with closed contours surrounding a single peak, as in Fig. 1b.

Analogous results are obtained when the spectrum index of the noise model $n(x)$ [Eq. (1)], is more general. Of particular interest for application to atmospheric turbulence data is the case $h = \frac{1}{3}$, corresponding through Eq. (2) to the Kolmogorov model or von Karman inertial range with spectrum proportional to $|\omega|^{-5/3}$. It can be verified that the analyzing wavelet illustrated in Fig. 2b—that is the smoothed difference filter—also satisfies the admissibility constraint [Eq. (9)] for this value of h. The associated discrete signal profile is found by solving Eq. (11) for $\bar{f}(x)$ with $W_h\bar{f}$ evaluated using Eqs. (6) and (10) and is shown in Fig. 2c. It can be seen that the signal profile (Fig. 2c) comprises a smooth increment similar to that in Fig. 2a but embedded in slowly-decaying tails.

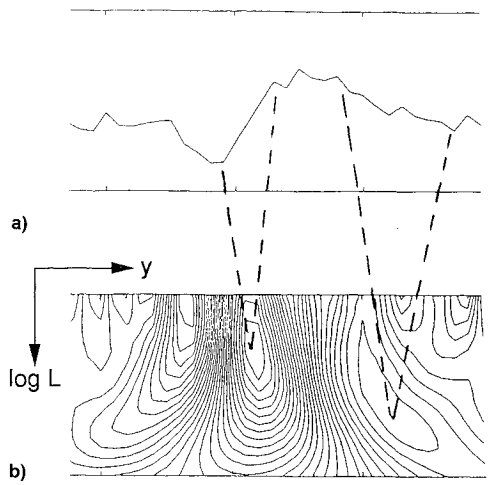

Fig. 3 a) Detail of measured sample of turbulence, and b) associated correlation surface.

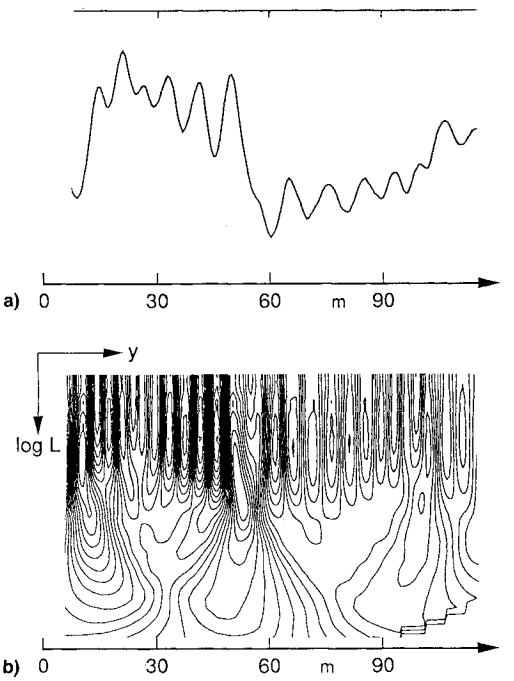

Fig. 4 a) Measured sample of turbulence, and b) associated correlation surface.

Fig. 3b shows the correlation surface [Eq. (4)] resulting from the application of the analyzing wavelet shown in Fig. 2b, using a scaling parameter $h = \frac{1}{3}$ to a short sample (Fig. 3a), of a measured turbulence velocity component. The association between peaks and troughs in the correlation surface and ramp-shaped increments in the measured record is illustrated, the longer ramp corresponding to a trough of a larger scale L.

A more detailed example processed in the same way is shown in Fig. 4. Particularly noticeable is the sequence of peaks and troughs in the correlation surface (Fig. 4b) associated with oscillatory structure in the measured record (Fig. 4a).

Alternative Expression for Correlation Surface

Equation (4) expresses the correlation surface $T_h(y, L)$ in terms of an analyzing wavelet $\bar{F}$. When $\bar{F}$ takes the particular form illustrated in Fig. 2b, $T_h(y, L)$ can be expressed alternatively as

$$T_h(y, L) = L^{-h} \int_{-\infty}^{\infty} H(x - y, L)\Delta g(x, L)\, \mathrm{d}x \tag{15}$$

where

$$\Delta g(x, L) = g(x + L/2) - g(x - L/2) \tag{16}$$

is a two-point difference of $g(x)$ taken over a distance L and $H(x, L)$ is a smoothing function of the shape illustrated in Fig. 1a which introduces a local average over a distance of order L. This result follows the fact that $\Delta g(x, L)$ [Eq. (16)] can be implemented as the convolution of $g(x)$ with a pair of delta functions—of opposite sign—separated by distance L.

Used in this form [Eq. (15)] the process of identifying peaks in $T_h(y, L)$ with the occurrence of discrete ramp gusts, typified by the profile in Fig. 2a, has been used[10,11] since the late 1960s and early 1970s as a standard method of turbulence analysis at the Royal Aerospace Establishment. More recently, published applications of the technique[12,13] have been concerned with its use to measure fractal dimensions. The application of the method as a basis for statistical analysis is discussed in the following section. The new aspect of the method (outlined in this article) concerns the explicit formulation of $T_h(y, L)$ in the form given in Eq. (4) in terms of signal detection theory.

Statistical Model for Discrete Gusts

It has been shown above that, with analyzing wavelet $\bar{F}(x)$ chosen to have the form illustrated in Fig. 2b, local maxima and minima in the position-scale correlation surface [Eq. (4)] can be identified with the occurrence of discrete events $f(x)$ in the form of ramp-shaped gusts. Assuming the discrete gusts $f(x)$ to be scaled versions of a single function $\bar{f}$

$$f(x) = m\bar{f}[(x - y)/L], \qquad (L > 0) \tag{17}$$

generalizing Eq. (3), their amplitude m, position y, and scale L can be estimated from the associated amplitude, position, and scale of the measured peaks (Figs. 3b and 4b).

A statistical description of the ensemble of discrete gusts $f(x)$ must take account of their density of occurrence, in position-scale space, and of their amplitudes. Stationarity is assumed with respect to position, and particular interest is focused on the dependence of both number density and amplitude on scale.

We denote by $N_{L,m}\,dL$ the average number per unit distance y, of discrete gusts [Eq. (17)] with scale in the range (L, $L + dL$) and amplitude greater than m. Note that $N_{L,m}$ is a density with respect to L but cumulative with respect to m. Separate distributions can be introduced for "up-ramps," corresponding to local maxima in the correlation surface, and "down-ramps," corresponding to local minima, but it is frequently convenient to combine these into one distribution.

Separate scaling laws for the number density $N_{L,m}$ and amplitude m are postulated[5] in the form

$$N_{L,m} \sim L^{-2} \cdot L^{1-D} = L^{-(1+D)} \tag{18}$$

$$m \sim L^{k} \tag{19}$$

The L^{-2} factor in Eq. (18) arises from the effect of scale on the number of correlation peaks per fixed (unit) y and fixed increment in scale dL, whereas the term L^{1-D} allows for possible intermittency in the sense that the fractal dimension $D(<1)$ of the set of points along the y axis that carry active fluctuations may be less than the dimension ($=1$) of the whole line. D is related[4] to the fractal dimension D^* of turbulent "eddies" in three-dimensional space by

$$D = D^* - 2, \qquad (D^* \leq 3) \tag{20}$$

It should be noted that the scaling laws [Eqs. (18) and (19)] introduced for the ensemble of discrete gusts $f(x)$ are quite distinct from the scaling parameter h assumed for the residual noise $n(x)$ [Eq. (2)]. Therefore, in principle, the two terms on the right side of Eq. (1) scale independently.

In the following, Eqs. (18) and (19) will be considered in three forms of increasing complexity. In the simplest case $D = 1$ and $k = \frac{1}{3}$. This corresponds to the traditional "self-similar" model of turbulence associated with the name of Kolmogorov. The second form occurs when $D < 1$ and $k < \frac{1}{3}$. This gives a "monofractal" model of turbulence of which a particular example is the "beta-model" of turbulence due to Frisch et al.[14] Finally we will consider the situation in which D and k are allowed to vary with discrete-gust amplitude. This leads to a "multifractal" model of turbulence as introduced by Parisi and Frisch.[15]

Statistical Analysis of Correlation Surface

The statistical model, incorporating scaling relationships of Eqs. (18) and (19) for the ensemble of discrete gusts $f(x)$ [Eq. (17)] provides a basis for the statistical analysis of the correlation surface $T_h(y, L)$ [Eqs. (4) and (15)].

The most direct approach is to generate the surface $T_h(y, L)$ as in Figs. 3b and 4b, using a value for the noise-scaling index h based on Eq. (2). A measured power spectrum of the data $g(x)$ [Eq. (1)] provides an initial estimate for the spectrum of the noise. Local maxima and minima in $T_h(y, L)$ can then be used to estimate positions, scales, and amplitudes of individual ramp gusts. The estimate of gust amplitude m is given by $L^h[T_h(y, L)]_{\max}$. If it is found that the measured index k [Eq. (19)] for the scaling of discrete gusts differs significantly from the value of h used to generate $T_h(y, L)$, it may be desirable to perform a second iteration with a revised value of h close to k, in order to keep the signal-to-noise ratio independent of scale.

However, as the evaluation of the correlation surface $T_h(y, L)$ on a two-dimensional (y, L) grid, and the subsequent identification and counting of peaks, is computationally expensive for large amounts of measured data, an equivalent method of analysis has been developed which requires only the calculation of the correlation surface along selected cross sections, at constant scale L, and the identification of peaks (local maxima and minima) on these cross sections, with respect to position y only. The principle underlying this method is that "position peaks" measured along lines of constant scale L reflect the existence of associated "position-scale peaks" (Fig. 4b), and that measurements of the statistical properties, including scaling, of the position peaks contain sufficient information as shown below to infer the statistical properties of the underlying ensemble of discrete gusts $f(x)$.

Since, from Eq. (4)

$$T_h(y, L) = L^{-h}T_0(y, L) \tag{21}$$

in order to investigate the y-variation of $T_h(y, L)$ for arbitrary h and fixed L, it is sufficient to study the y-variation of $T_0(y, L)$ at the same L. This has the advantage of allowing position peaks to be identified without the need for prior information concerning h.

At scale L the cumulative number per unit distance y of position peaks in the function $T_0(y, L)$ with magnitude greater than z will be denoted by $n(L, z)$. The scaling properties of $n(L, z)$ can be deduced by considering the influence of the ensemble of discrete gusts satisfying Eqs. (18) and (19). This problem is a particular case of the general theory presented in Ref. 5 for the effects of the ensemble of discrete gusts on an arbitrary linear filter. Applied to the filter $T_0(y, L)$ and assuming that the signal-to-noise ratio is sufficiently high for the effects of noise $n(x)$ [Eq. (1)] on the amplitude of the peaks to be neglected, the results in terms of scaling laws are

$$n(L, z) \sim L^{-D} \tag{22}$$

$$z \sim L^{k} \tag{23}$$

Thus, with the appropriate choice of exponents D and k, a plot of $L^D n(L, z)$ against z/L^k will give a scale-invariant curve.

In fact, Ref. 5 goes beyond the step of establishing scaling laws and through an application of the Laplace asymptotic approximation, shows how a measurement of the above-scale-invariant distribution allows the numerical constants of proportionality implied by Eqs. (18) and (19) to be derived, and therefore, an explicit statistical-discrete-gust model[5-7] to be fitted to the data.

Analysis of Measured Data

The analysis method outlined above is applied in the following to samples taken from measured records of atmospheric turbulence obtained[16] using a specially-instrumented aircraft at altitudes below 1000 ft over a variety of types of terrain in the United Kingdom. Details of the instrumentation and data processing, together with an assessment of the extracted turbulence measurements, have been presented in a previous article.[17]

For these flight measurements a detailed statistical discrete-gust analysis, based on Eqs. (22) and (23) with scaling indices $D = 1$, $k = \frac{1}{3}$ (the classical self-similar model), has been presented in Ref. 17 and compared with the results of power-spectral-density methods. It was concluded[17] that this model

gives (for practical aeronautical-engineering purposes) an adequate representation of turbulence structure at the lower range of amplitudes which (expressed in terms of spatial increments in turbulence velocity) extends up to about four times the rms value but excludes the more intense fluctuations.

Illustrated in Ref. 13 were the results of analyzing a particular sample of turbulence from these flight measurements using the self-similar model ($D = 1$, $k = \frac{1}{3}$) and also using the more general (mono)fractal model with the indices D and k treated as independent free parameters. Plots of $S^D n(L, z)$ against z/L^k showed that for this sample an improved fit of the model to the data was achieved at the larger amplitudes with empirically-fitted exponents $D = 0.45$ and $k = 0.23$. These numerical values are quoted here not as reliable estimates, but rather as typical of those obtained in a wider study. Considerable scatter in the estimated exponents occurs between different measured samples.

However, in a detailed statistical study[18] of flight-measured data pooled from over 400 individual samples of the lateral component of turbulence velocity, the same method of analysis has been applied systematically over various bands of gust amplitude. Figs. 5a–c show the measured cumulative number $n(L, z)$ of peaks in the function $T_0(y, L)$ exceeding threshold z for a range of L from 5.7 to 45.2 m. Axes are scaled according to Eqs. (22) and (23). Values of D range from 1 (in Fig. 5a) to 0.5 (Fig. 5c). Associated values of k range from $\frac{1}{3}$ to $\frac{1}{6}$.

It can be seen (Fig. 5a) that when $D = 1$, $k = \frac{1}{3}$ (the basic self-similar model) the data collapse quite well onto a single curve at the lower levels of z. However, when D and k are reduced to 0.7 and 0.23, respectively (Fig. 5b), the range over which the data collapse is extended to higher amplitudes, whereas the degree of collapse is degraded at the lowest amplitudes. A measurement of least-squares variation shows that the degree of collapse at the highest amplitudes near the tails is further improved if D and k are reduced to 0.5 and $\frac{1}{6}$ (Fig. 5c), although a deterioration in the quality of statistical data collapse is to be expected on the tails of the distribution where the size of the data sample is necessarily small.

We draw the conclusion from Fig. 5 that the best overall model of turbulence is multifractal,[12,15] the scaling index k reducing from its classical value of $\frac{1}{3}$ at the lower amplitudes to a reduced value closer to $\frac{1}{6}$ at the highest gust intensities.

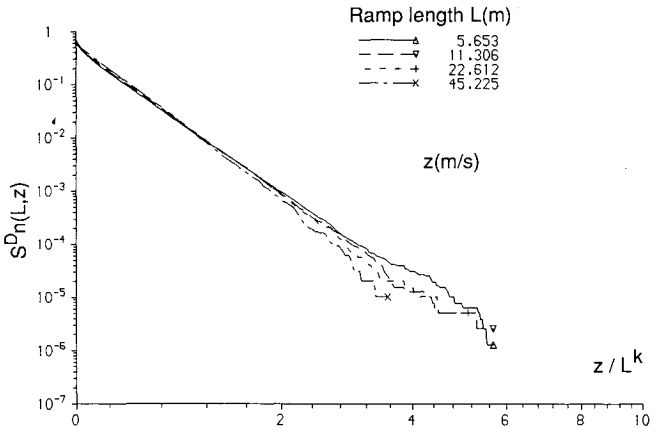

a) $D = 1$ ($D^* = 3$), $k = \frac{1}{3}$

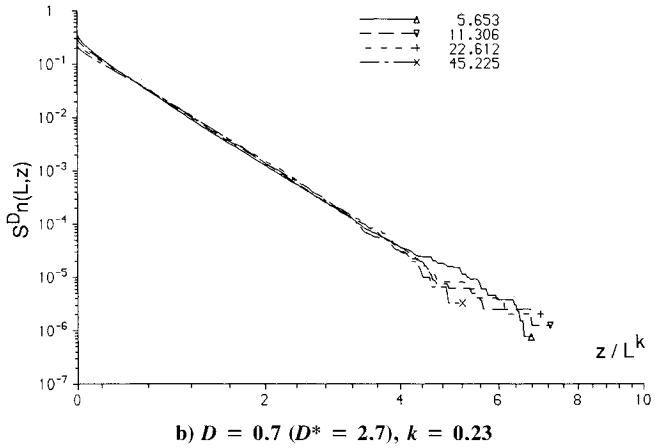

b) $D = 0.7$ ($D^* = 2.7$), $k = 0.23$

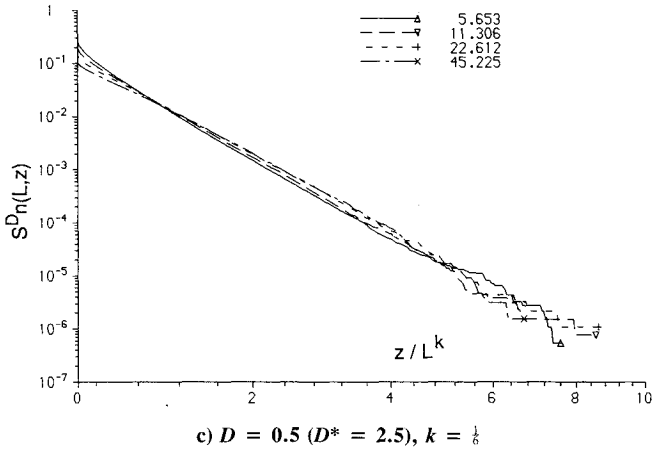

c) $D = 0.5$ ($D^* = 2.5$), $k = \frac{1}{6}$

Fig. 5 Flight-measured data scaled using fractal indices (lognormal-based axes)

Implications for Aircraft Design Criteria

The overall trend in the results described in the previous section is that, although a value of the fractal dimension D close to unity ($D^* = 3$) gives a good match to the data at the lower gust amplitudes, decreasing estimates of D compatible with an asymptotic value $D \doteqdot 0.5$ ($D^* \doteqdot 2.5$) are obtained as the amplitude band moves to higher intensities. These results are consistent with previous estimates[4] of D^*, in the range 2.8–2.5. Over the same range, the corresponding estimated value of the scaling index k reduces from $\frac{1}{3}$ to a value closer to $\frac{1}{6}$.

In the fractal model with $D = 0.5$ ($D^* = 2.5$) and $k \doteqdot \frac{1}{6}$ (compatible with the experimental results at the highest gust intensities) there is a trend in which the intermittency increases with decreasing scale L. At the smaller scales the localized events, or discrete gusts, are fewer in number, but larger in amplitude, than would be the case in a self-similar model ($k = \frac{1}{3}$). For example, given a reference gust, e.g., $L = 100$ m, a change from the $k = \frac{1}{3}$ to the $k = \frac{1}{6}$ law implies a relative increase in the amplitudes of the gusts for which $L < 100$ m. As the $k = \frac{1}{3}$ law is implicit[5] in power-spectral-density (PSD) methods, as applied in the inertial range of the standard von Karman power spectrum, it also follows that the shorter gusts are more intense than would be expected if the scaling of their amplitudes were to be based simply on a knowledge of the PSD.

These results have important implications[13] for the prediction of structural loads and the performance of load-alleviation control systems, for each of which gusts with scale L less than 100 m can be critical. The correct representation in aircraft design criteria of short gusts is of particular relevance to modern technology aircraft which use powerful active-control systems, as the effect of such systems is sometimes to reduce the scale L of the gusts to which the aircraft predominantly responds.[19] This is true, in particular, of direct lift control (DLC) systems. In Ref. 20, e.g., it is shown that whereas the reduction of gust-induced fluctuations in aircraft normal acceleration and associated loads by increases in wing loading or reductions in lift-curve slope also produces an increase in the gradient distance of the tuned gust, analogous reductions in normal acceleration by the use of DLC are accompanied by a decrease in the tuned gradient distance.

Concluding Remarks

A form of Wavelet decomposition has been described which, when applied to turbulence, extracts localized structure in the form of discrete ramp-shaped gusts. Pictorial representations of the position-scale correlation surface (Figs. 3b and 4b) illustrate graphically the discrete-gust content in the form of local peaks and troughs. It has been shown how a statistical analysis of peaks identified in the correlation surface can be used to fit a statistical discrete-gust model, which incorporates fractal scaling exponents, to measured data. Trends in the results, which indicate that short gusts are of a greater amplitude than would have been predicted using a classical self-similar model or power-spectral-density analysis, have been discussed in terms of their relevance to aircraft design criteria.

Acknowledgment

The correlation surface in Fig. 4 was computed using a software implementation due to G. H. Watson, of SD-Scicon (UK) Ltd.

References

[1]Grossman, A., and Morlet, J., "Decomposition of Functions into Wavelets of Constant Shape, and Related Transforms," *Mathematics and Physics, Lectures on Recent Results*, Vol. 1, edited by L. Streit, World Scientific, Singapore, 1985, p. 320.

[2]Kronland-Martinet, R., Morlet, J., and Grossman, A., "Analysis of Sound Patterns Through Wavelet Transforms," *International Journal of Pattern Recognition and Artificial Intelligence*, Vol. 1, No. 2, 1987, pp. 273–302.

[3]Jones, J. G., Earwicker, P. G., and Foster, G. W., "Multiple-Scale Correlation Detection, Wavelet Transforms and Multifractal Turbulence," IMA Conf. on Wavelets, Fractals and Fourier Transforms, Newnham College, Cambridge, England, UK, Dec. 1990.

[4]Mandelbrot, B. B., *The Fractal Geometry of Nature*, WH Freeman, San Francisco, CA, 1977, 1982, p. 460.

[5]Jones, J. G., "Statistical-Discrete-Gust Method for Predicting Aircraft Loads and Dynamic Response," *Journal of Aircraft*, Vol. 26, No. 4, 1989, pp. 382–392.

[6]Jones, J. G., "The Statistical Discrete Gust (SDG) Method in its Developed Form," AIAA 30th SDM Conf., AIAA Paper 89-1375, Mobile, AL, April 3–5, 1989, pp. 1892–1898.

[7]Jones, J. G.,"A Unified Procedure for Meeting Power-Spectral-Density and Statistical-Discrete-Gust Requirements for Flight in Turbulence," AIAA 27th SDM Conf., AIAA Paper 86-1011, San Antonio, TX, May 19–21, 1986, pp. 646–652.

[8]Jones, J. G., and Haynes, A., "A Peakspotter Program Applied to the Analysis of Increments in Turbulence Velocity," Royal Aircraft Establishment, TR-84071, Farnborough, England, UK, July 1984.

[9]Foster, G. W., and Jones, J. G., "Measurement and Analysis of Low Altitude Atmospheric Turbulence," AGARD Rept. R-734, Paper 2, Farnborough, England, UK, Dec. 1987.

[10]Jones, J. G., "Similarity Theory of Gust Loads on Aircraft, Development of Discrete Gust Theory," Royal Aircraft Establishment, TR-69171, Farnborough, England, UK, Aug. 1969.

[11]Jones, J. G., "Statistical Discrete Gust Theory for Aircraft Loads," Royal Aircraft Establishment, TR-73167, Farnborough, England, UK, Oct. 1973.

[12]Jones, J. G., "On Self-Similarity, Fractal Dimension and Aircraft Response to Gusts," Royal Aircraft Establishment, TM FS-244, Farnborough, England, UK, March 1979.

[13]Jones, J. G., Foster, G. W., and Haynes, A., "Fractal Properties of Inertial Range Turbulence with Implications for Aircraft Response," *Aeronautical Journal of the Royal Aeronautical Society*, Vol. 92, Oct. 1988, pp. 301–308.

[14]Frisch, U., Sulem, P.-L., and Nelkin, M., "A Simple Dynamical Model of Intermittent Fully Developed Turbulence," *Journal of Fluid Mechanics*, Vol. 87, Pt. 4, 1978, pp. 719–736.

[15]Parisi, G., and Frisch, U., "A Multi-Fractal Model of Intermittency," *Turbulence and Predictability in Geophysical Fluid Dynamics and Climate Dynamics*, edited by M. Ghil, R. Benzi, and G. Parisi, North-Holland, Amsterdam, 1985, pp. 84–88.

[16]Foster, G. W., "Results of Low Altitude Atmospheric Turbulence Measurements," Royal Aircraft Establishment, TR-87015, Farnborough, England, UK, Feb. 1987.

[17]Foster, G. W., and Jones, J. G., "Analysis of Atmospheric Turbulence Measurements by Spectral and Discrete-Gust Methods," *Aeronautical Journal of the Royal Aeronautical Society*, Vol. 93, No. 925, 1989, pp. 162–176.

[18]Jones, J. G., Foster, G. W., and King, M., "Multifractal Scaling of Measured Increments in Atmospheric Turbulence Velocity" (paper in preparation).

[19]Jones, J. G., "Design of Control Laws to Implement ACT Benefits," *Aeronautical Journal of the Royal Aeronautical Society*, Jan. 1980, pp. 13–21.

[20]Jones, J. G., and Fry, D. E., "Ride-Bumpiness in High-Speed Flight at Low Altitudes," *Aeronautical Journal of the Royal Aeronautical Society*, Vol. 93, No. 926, 1989, pp. 219–228.